22nd Biennial Conference on Mechanical Vibration and Noise
2009 IDETC/CIE
Aug. 30-Sept. 2, 2009, San Diego, California, USA

PARAMETER IDENTIFICATION OF A CANTILEVER BEAM IMMERSED IN VISCOUS FLUIDS WITH POTENTIAL APPLICATIONS TO THE PROBE CALIBRATION OF ATOMIC FORCE MICROSCOPES

Wenlung Li and S. P. Tseng
Dept. of Mechanical Engineering
National Taipei University of Technology
Taipei 106, TAIWAN

ABSTRACT

The main objective of the report is to present a new identification method has been derived for single-degree, base-excited systems. The system is actually to mimic a probe of cantilever type of AFMs. In fact, the idea of the present report was initiated by needs for *in situ* spring constant calibration for such probe systems. Calibration processes can be treated as parameter identification for the stiffness of the probe before it is used. However, sine a real probe is too small to be seen by bare eyes and too costly to verify, a cantilever beam was adopted to replace it during the study. The present method starts with giving a chirp excitation to the target system, and to lock the damped natural frequency. Once the damped natural frequency is obtained, it is possible to locate the frequency at which the phase lag is equal to $\pi/2$. From which, the excitation frequency is then purposely changed to that frequency and the corresponding steady-state responses are measured. In the meantime, the system dissipative energy or power may also need to be stored. In fact, the present identification formulation is to express the spring constant of the target systems in terms of two measurable parameters: the phase angle and the system damping. The former can be computed from the damped natural frequency while the latter can be identified along with measuring the input power. The novel formulation is then numerically simulated using the Simulink toolbox of MATLAB. The simulation results clearly showed the current identification method can work with good accuracy. Following the numerical simulation, experimental measurements were also carried out by a cantilever beam that its free end was immersed to viscid fluids. The fluids of different viscosity were used to mimic the environments of a probe in use. The experimental results again substantiated the correctness of the present method. Thus it is accordingly concluded that the new recognition algorithm can be applied with confidence.

INTRODUCTION

Calibration of the spring constant for the cantilever probe of atomic force microscopes (AFM) is necessary for lots of applications. And there is an increasing need for the accurate measurement of small forces, particularly for researches in surface science. Using a probe without careful calibration or direct applying the data from suppliers normally leads to very large errors in force measurements. During the last decade, a number of calibration methods have been developed and reviewed [1] for calibration of various applications. In general, those calibration methods for a cantilever probe may be divided into a few major approaches based on their technical principles. They include like methods using geometric dimensions together with FEA, dynamic or static response methods, comparison with a reference quantity, and thermal noise methods, etc.

Methods using the physical dimensions as well as material properties may be the simplest, even though they may not be the most accurate ones. By applying the well-known Euler-Bernoulli beam theory, it is possible to obtain a reasonable spring constant for that cantilever probe. However, since probes are made by utilizing an MEMS process, the physical dimensions are not as homogenous as one has expected. For example, the thickness of cantilevers, which are in cubic relation to the spring constant, may result in as high as 50% error [2]. Hence, applying one of these methods may be a good reference but not that practical. In addition, to measure the true dimensions of a probe, compute its spring constant, and then mount it on the probe clip seems to increase the possibility of damaging that probe. However, [3] has applied such calibration method for rectangular cross-section ones. He obtained less than 2% error when comparing with that obtained from an electrostatic force balance. In addition, [4] suggested that non-rectangular cross-section can also apply these methods if an equivalent cross-sectional area is considered.

Most dynamic response methods mainly focus at the measurement of resonant frequency of cantilever probes. Combining measurements of physical dimensions and other material properties, one is able to the approximate mass of the beam. From them, it is possible to calculate the spring constant of that cantilever probe. For example, the so-called Sader methods [5] are actually of this kind. Considering the calibration procedures, there are two possible blunders in addition the errors from geometric measurements: (1) The measured resonant frequency should be the damped one. However, it has been regarded as the natural frequency, even though their differences are small if the system is lightly damped. And (2) model error results from the lumped mass [6] and from the photo reflecting in which the vertical oscillation can hardly be measured. The discrepancy may as high as 33% according to [7].

Using a known quantity as the reference, one is to measure the other affected quantities by putting this reference onto the cantilever beam. For instance, [8] put an additional mass to the beam and measured the change of beam natural frequency. From the relation of the original mass and added mass, it is possible to obtain the spring constant of the original cantilever probe. The advantage of such methods stems from no need to have material properties, particularly the Young's modulus of the beam. However, to correctly measure and put the additional mass to the right location normally become difficulties of calibration [9]. Besides, it can scarcely be applied after the probe is mounted in place. Another group of these methods carry out their calibration by using a probe whose spring constant has been known a priori [10, 11], or the so-called "dual probe calibration." In spite of possibility of damaging the probe to be calibrated, [12] reported that it can be used only for limited range of cantilever stiffness. Not to mention that it has only ±10 ~ 20% relative precision [12] by using such calibration. In addition, such calibration procedure may be regarded as a static loading one. Therefore, an alternative of non-contact force may be more attractive instead of contact forces.

To calculate the thermal noise induced vibrations in accordance with the equi-partition theorem is the basic idea for such calibrations. The equi-partition theorem states that if a system is in thermal equilibrium, every independent quadratic term in its total energy has a mean value equal to one half of ($\kappa_B \times T$), where κ_B is the Boltzman constant, and T the absolute temperature. For example, a cantilever beam of 50 mN/m spring constant approximately has its thermal oscillation amplitude in 3 Å. Using methods are quite like the on-line calibration. However, it may be good for small spring constant beams, according to [9, 13]. In addition, it may need to several modes in addition to the first one, since thermal energy inspires all modes simultaneously. In case of taking only one mode, it may result in error as high as 30% [14, 15].

In addition to the upper mentioned ones, other calibrations are also reviewed, such as nano-indentation methods [e.g., 16], and intrinsic methods [e.g., 4]. Ref. [1] has provided a very good review and comments for those methods. Readers are referred to that report. After reviewing these calibration methods, the authors would summarize that a practical method should be (1) reliable, (2) easy and low cost to apply, and (3) no damage to the probe. And more importantly, it can be applied after the probe is mounted to the holder clip. However, it seems to the authors that this calibration procedure still awaits to be developed. Motivated by this, the present report is attempting to derive an on-line calibration method via the dynamic responses of probe. Since the probe of an AFM is too small to verify, the present report replaces the probe with a cantilever beam to mimic the real probe system.

DERIVATION OF THE METHOD

Figure 1(a) shows the schematic diagram for the signal detection system of an AFM, consisting of a cantilever probe together with its bimorph actuator. The system may be modeled by a linear SDOF system with a based excitation, shown in Fig. 1(b), if only the first mode of the cantilever is interested. During the calibration process, the probe is applied an external voltage with varying frequency close to the first mode of the cantilever to drive the bimorph so that the probe is oscillating in air. The absolute oscillating response, $z(t)$, manly due to the first mode of the cantilever can be represented by

$$m\ddot{z} + c(\dot{z} - \dot{u}) + k(z - u) = 0\,, \qquad (1)$$

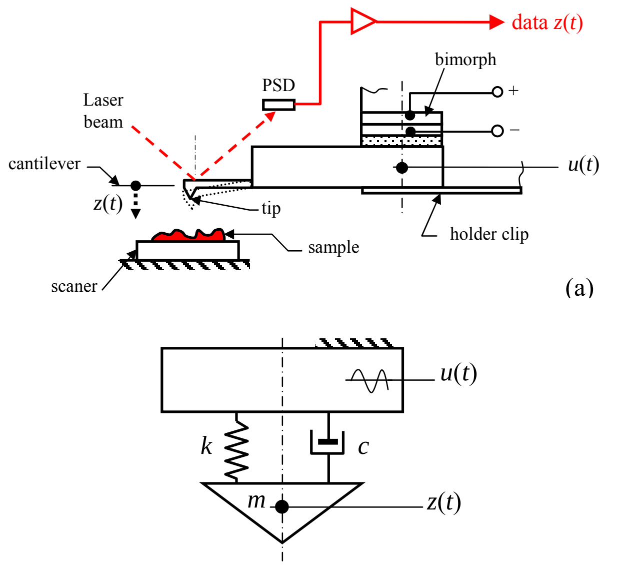

(b)

Fig. 1. (a) Schematic diagram of the optical lever detection system for an AFM; and (b) its dynamic model of the fist mode.

if the excitation from the bimorph is $u(t)$, where m, c, and k are the equivalent mass, damping and stiffness of the cantilever, respectively. The steady-state solution of eqn (1) for the tip oscillation $z(t)$ can be thus obtained as in the complex form

$$z(t) = Ze^{i(\Omega t-\phi)}, \tag{2}$$

if the bimorph excitation displacement satisfies

$$u(t) = Ue^{i\Omega t}, \tag{3}$$

in which ϕ is the phase angle. Obviously, $z(t)$ in eqn (2) can be expressed as the function of $u(t)$, i.e.,

$$z(t) = \left[\frac{1+i(2r\varsigma)}{(1-r^2)+i(2r\varsigma)}\right]U\, e^{i\Omega t}, \tag{4}$$

where

$$\varsigma = \frac{c}{2\sqrt{mk}}, \quad r = \frac{\Omega}{\omega_n} \quad \text{and} \quad \omega_n^2 = \frac{k}{m} \quad . \tag{5}$$

The amplitude of the absolute oscillation of tips can be also defined in terms of the transmissibility, which denotes the portion of the bimorph input that has been transmitted to the output (probe), cf. eqn (4), one writes

$$Z = T_z \cdot U, \tag{6}$$

and

$$T_z(r,\varsigma) = \left[\frac{1+(2\varsigma\, r)^2}{(1-r^2)^2+(2\varsigma\, r)^2}\right]^{1/2}. \tag{7}$$

On the other hand, the phase lag due to system damping in eqn (2) can also be expressed as

$$\begin{aligned}\tan\phi &= \frac{m\, c\, \Omega^3/\Lambda}{[k(k-m\Omega^2)+(\Omega c)^2]/\Lambda} \\ &= \frac{(2\varsigma\, r^3)}{[(1-r^2)+(2r\varsigma)^2]}\end{aligned} \tag{8}$$

where

$$\Lambda = (k-m\Omega^2)^2+(\Omega c)^2 = k^2\left[(1-r^2)^2+(2r\varsigma)^2\right]. \tag{9}$$

Examining eqns (7) and (8), the transmissibility and the phase lag are function of r and ς, and cannot be known unless the correct damping ratio is precisely measured *a priori*.

In order to identify the damping ratio of a structural system, several methods have been developed by the first author [e.g., 17], in addition to a lot of ones. Here, however, one is to apply an excitation with its frequency Ω in such way that the phase angle ϕ is purposely equal to $\pi/2$ (or 90°). That is, let the frequency where $\phi = \pi/2$ be ω_0, i.e., the present method is to urge the experimenter to set $\Omega = \omega_0$ in eqn (8). Under this circumstance, the denominator of eqn (8) is actually $\cos\phi$, and hence $\cos\phi \to 0$ at $\Omega = \omega_0$. Or, the denominator of eqn (8) has to satisfy

$$(1-r_0^2)+(2r_0\varsigma)^2 = 0, \tag{10}$$

where $r_0 = \omega_0/\omega_n$. Or, equivalently

$$\frac{\omega_0}{\omega_n} = \frac{Q}{\sqrt{Q^2-1}}, \tag{11}$$

since

$$\omega_\mathrm{d}/\omega_n = \sqrt{1-\varsigma^2} \quad \text{and} \quad Q = \frac{1}{2\varsigma}. \tag{12}$$

where Q is the system quality factor. Here, one has defined ω_d is the so-called damped natural frequency, which can be experimentally measured by a chirp or wide-band excitation.

On the other hand, because the present method requires the frequency of the external excitations to be exactly at ω_0, the phase angle must satisfy $\tan\phi \to \infty$. Equivalently, it mathematically means that not only the denominator of eqn (8) must be zero, but also the numerator has to be an arbitrary non-zero constant. Therefore, one writes

$$\begin{cases} \dfrac{m\, c\, \omega_0^3}{(k-m\,\omega_0^2)^2+(\omega_0 c)^2} = \sqrt{\alpha} \\ k(k-m\,\omega_0^2)+(\omega_0 c)^2 = 0 \end{cases} \tag{13}$$

in which α represents an unknown, non-zero, real constant. Solving eqn (13), one at least can have a set of solution that satisfies

$$k = \frac{c\cdot\omega_0}{\sqrt{\alpha}} \quad \text{and} \quad m = \frac{c(1+\alpha)}{\omega_0\sqrt{\alpha}}. \tag{14}$$

By using equation (5) which is the definition of the natural frequency or the ratio of k to m, one follows that the arbitrary constant α in (13) must be

$$\alpha = \frac{1}{Q^2-1} \tag{15}$$

Substituting this expression back into eqn (14), this allows one to identify the probe spring constant k, in addition to m as a function ω_0:

$$k(\omega_0) = c\cdot\omega_0\sqrt{Q^2-1} \quad . \tag{16}$$

The formulation in eqn (16) is exact and good for $\Omega = \omega_0$. To the best of authors' knowledge, this expression has not been attempted in literature. And the formulation is an "almost" close form, since the only assumption made is in eqn (12) for the quality factor through the derivation. Alternately, one may writes the estimated spring constant k in eqn (16) in terms of ω_d which can be directly measured as

$$k(\omega_d) = c\cdot\omega_d\left(\frac{2Q^2}{\sqrt{4Q^2-1}}\right). \tag{17}$$

Unfortunately, notice that from either eqn (16) or (17), one can experimentally or indirectly obtain all parameters on RHS except system damping c. Or, unless the probe damping is known, the two expressions, both involve one unknown, are not much helpful in identifying system stiffness. Thus, one has to recognize the system damping prior to estimate the spring constant.

2.1 SYSTEM DAMPING: DISSIPATIVE ENERGY

Theoretically, the total energy involves in every $z(t)$ cycle of probe oscillations may be obtained by integrating eqn (1). Or,

$$\Delta E = \oint [m\ddot{z} + c(\dot{z} - \dot{u}) + k(z-u)] \cdot dz \, . \tag{18}$$

The o-integral in the upper equation denotes the integration is done for a complete $z(t)$ cycle. Replace dz by $\dot{z}\,dt$ in eqn (18) and integrate from 0 to 2π/Ω, one is able to compute Δ*E*. For the reason of simplicity, one lets input excitation for eqn (2) be sinusoidal of the form

$$u(t) = U \sin(\Omega t) \, . \tag{19}$$

Hence, from eqn (3) $z(t)$ becomes

$$z(t) = T_z U \cdot \sin(\Omega t - \phi) \, . \tag{20}$$

Furthermore, applying eqns (19) and (20) to (18), one has the form

$$\Delta E = c\pi (T_z U)^2 \Omega + c\pi (T_z U^2)\Omega \cos\phi - k\pi (T_z U^2)\sin\phi \, , \tag{21}$$

for the total involved energy of every oscillation cycles. Examining the upper equation, the third term on the RHS is strain energy from the relative motion of $u(t)$ to its response $z(t)$. Or, the cantilever spring can only deliver the energy to the tip once the probe system is in steady-state. Thus, this energy does not dissipated away in steady state. The second term to the RHS is regarded as the damped energy from these relative motions. Similarly, the first term to the RHS also dissipates energy away due to the probe damping. In the meantime, the energies of these two terms have to be externally made up so that the oscillation can keep up during steady-state. As a result, the total dissipative energy, that has to be externally supplied, per cycle can be expressed by

$$\Delta E_d(\Omega) = c\pi (T_z U)^2 \Omega + c\pi (T_z U^2)\Omega \cos\phi \, , \tag{22}$$

in case of steady-state oscillations. To simplify equation (22), recall from eqn (13) that one has set the external frequency $\Omega = \omega_0$. That is, $\cos\phi = 0$, or eqn (22) can be further simplified as

$$\Delta E_d(\omega_0) = c\pi\omega_0 \cdot (T_z U)^2 \, . \tag{23}$$

Note that eqn (18) has reported a way to measure the dissipative energy via the product modulations of the input and output signals. This may be a good alternative in addition to direct measuring. Besides, the input power (or energy) must be equal to the system dissipated energy ΔE_d during the steady-state. In other words, this makes it possible to measure the system dissipated energy externally. Thus, for now, one just re-arranges eqn (23), and using the averaged dissipative power $\Delta p_0 = (\omega_0 \Delta E_d)/2\pi$, the system damping c can be solved as

$$c = \frac{2\,\Delta p_0}{Z_0^2 \cdot \omega_0^2} \, . \tag{24}$$

where $T_Z U$ has been replaced by the probe response amplitude Z_0 since the latter is easier to be measured at $\Omega = \omega_0$. Notice that the parameters on the RHS of eqn (24) are all measurable. Obviously, the accuracy of parameter estimation depends on how accurate the three parameters on RHS can be measured. Nevertheless, damping c can be experimentally determined. Using the upper eqn (24) to (16), the close form, with all *in situ* measurable parameters, of the estimated probe stiffness becomes

$$\hat{k} = \frac{2\,\Delta p_0}{Z_0^2 \cdot \omega_0} \cdot \sqrt{Q^2 - 1} \, . \tag{25}$$

2.2 ERROR ANALYSES

Assuming the energy (ΔE_d or Δp_0) dissipated from the system can be correctly measured, while the quality factor (Q) may have certain amount of error ΔQ, then the identified spring constant of probes represented in eqn (25) may be written in terms of the Taylor expansion around its correct value (Q_0). That is to express $Q = Q_0 - \Delta Q$ to eqn (25) and write

$$\hat{k} = \frac{2\,\Delta p_0}{Z_0^2 \cdot \omega_0} \sqrt{Q_0^2 - 1} \left(1 + \frac{Q_0 \cdot \Delta Q}{Q_0^2 - 1} - \frac{\Delta Q^2}{2(Q_0^2 - 1)^2} + O(\Delta Q^3) \right) . \tag{26}$$

One further lets $\Delta Q / Q_0 = \varepsilon_Q$, eqn (26) becomes

$$\hat{k} = k_0 \left(1 + \frac{\varepsilon_Q}{1 - (1/Q_0^2)} - \frac{\varepsilon_Q^2}{2[1 - (1/Q_0^2)]^2} + O(\varepsilon_Q^3) \right) . \tag{27}$$

Thus, eqn (27) depicts that the error of the estimated spring constant is linearly w.r.t the error of system quality factor. Similarly, if one considers ω_0 to have ε_ω relative error in addition to ε_Q. By neglecting all higher order terms, eqn (27) may be expressed as the function of ε_ω and ε_Q:

$$\hat{k} = k_0 \left(1 + \frac{\varepsilon_Q}{1 - (1/Q_0^2)} - \frac{\varepsilon_Q^2}{2[1 - (1/Q_0^2)]^2} \right) \left(1 - \varepsilon_\omega + \varepsilon_\omega^2 \right) + O(\varepsilon_Q^3, \varepsilon_\omega^3) \, . \tag{28}$$

Or,

$$\hat{k} \doteq k_0 \left(1 + \varepsilon_Q - \frac{\varepsilon_Q^2}{2} \right) \left(1 - \varepsilon_\omega + \varepsilon_\omega^2 \right) \tag{29}$$

if Q is large enough, which is normally true for AFM probes. Figure 2 shows numerical results. It shows that over-estimate the quality factor Q together with under estimate ω_0 tends to be a larger error in spring constants.

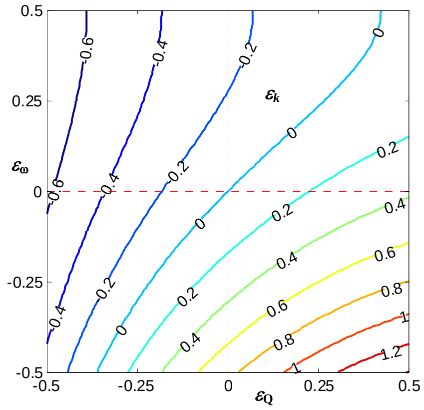

Fig. 2 Error trends of estimated spring constants.

In addition to the error sources from the estimated quality factor Q and the frequency location ω_0, one other possible error source may be from the measurement of the dissipative power or energy. Refer to Fig. 1, it is quite clear that the bimorph actuator of probes also dissipates away certain amount of energy during beam oscillations, mostly due to the material damping of bimorphs. Fortunately, this can be reasonably measured before probes are mounted onto the clip. In other words, one is first to calibrate the power consumed at ω_0 without a probe, i.e., by the bimorph itself. Let the power without a probe be ΔP_{b0} and remain constant for the whole period of stiffness detection. And also let the total power dissipated after probes mounted be ΔP_{total}. Then, one is able to obtain a good estimation of the dissipative power for the probe cantilever itself by subtracting the two [19]:

$$\Delta P_0 = \Delta P_{total} - \Delta P_{b0} \tag{30}$$

if the air friction to the beam is relatively negligible. Otherwise, the product modulation method [20] can be a good alternative.

VERIFICATION BY NUMERICAL SIMULATIONS

Numerical simulations using the commercial package, MATLAB Simulink toolbox, were carried out for confirmation of the theoretical derivation in the former section. The main objective was to ensure those formulations could properly work for various damped environments. However, since the size of probes for a real AFM is too small to see or to verify by bare eyes, the experiment was designed to carry out by a cantilever beam that mimics the real AFM probe. Anticipating the size of later experiments, to verify the current calibration method, the following system parameters with consistent units, were freely given: m = 0.06, c = 0.10 ~ 8.0 (ca. equivalent to ς = 0.2 % ~ 13.3 %), and the system natural frequency f_n was set to around 80 Hz, i.e., to fix the spring constant at k = 1.50e04. The Simulink model, as shown in Fig. 3, was established to identify these given values.

Simulating the calibration procedures, one started with finding the natural frequency of the beam. A chirp signal, from 3 to 250 Hz in 3 sec, was adopted to scan the damped natural frequency here. The sampling frequency f_s and sampling time T were 2 kHz and 5 sec, respectively. Once the damped natural frequency of the cantilever system was locked, the location of ω_0 can be easily computed. Following the chirp excitation, the excitation was then changed to ω_0 so that the steady-state responses under that excitation were properly recorded for later analyses. In the meantime, it had assumed that the dissipative energy could be correctly measured, while it can be calculated from the model. The results are given in Table 1 where the notations with over-hat denote estimated values.

It can be seen clearly from the table that quite small percentage of errors for estimated stiffness ε_k. Even when the error in the quality factor, ε_Q, is as large as ca. +6.19 %, the present identification method still can correctly recognize the probe stiffness with acceptable amount of errors (+5.18 %). Notice also that it has a trend that the larger damping tends to have a lager error in stiffness estimation. This may mainly stems from the approximate form of the Q-sharpness factor in eqn (12). Furthermore, when system damping is small, the estimated error for stiffness also tends to increase. However, the reason is because that discrete numerical simulation is normally hard to accurately locate their peaks when system responses are very sharp. This is somehow different from those of larger damping. In addition, this also implies that an analog circuit may be needed to apply the present calibration method to the probe system of AFM for vacuum environments.

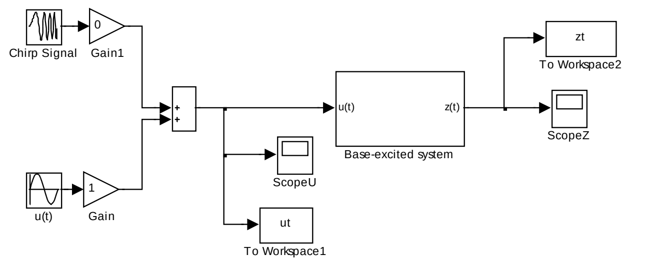

Fig. 3 The Simulink model for numerical verifications.

Table 1 Simulation results for k = 1.50E+4 (T = 5 sec).

Damping		Spring Constant		Frequency		Quality factor		
c	ς(%)	$\hat{k}$	ε_k(%)	$\hat{\omega}_0$(Hz)	ε_ω(%)	$Q_0(1/2\varsigma)$	$\hat{Q}$	ε_Q(%)
0.10	0.20	1.4465E+4	−3.57	79.601	−0.02	294.17	289.11	−1.67
0.25	0.42	1.5010E+4	+0.07	79.604	−0.02	119.04	120.06	+0.84
0.5	0.83	1.5033E+4	+0.22	79.614	−0.02	60.24	60.12	−0.20
1	1.67	1.5064E+4	+0.43	79.655	−0.01	29.94	30.12	+0.59
2	3.33	1.5097E+4	+0.65	79.618	−0.22	15.02	15.13	+0.74
4	6.67	1.5262E+4	+1.75	80.056	−0.35	7.50	7.66	+2.12
6	10.0	1.5559E+4	+3.73	81.091	−0.21	5.00	5.19	+3.77
8	13.3	1.5777E+4	+5.18	81.431	−1.42	3.75	3.98	+6.19

EXPERIMENTAL VALIDATION

In addition to the numerical verifications given in the last section, several experimental measurements were carried out. The main objective of the experiments is to verify the validity of eqn (16) or (17). The experimental setup for the measurements is shown in Fig. 4. The test specimen was an austenite stainless steel (Young's modulus E = 210 GPa) cantilever with dimensions $1.6^T \times 20.2^W \times 194^L$ mm (ca. 45.68 g) directly mounted to a shaker by a bolt. At the end of the beam, it was a plastic straw with the length 96 mm and the outer diameter 8.6 mm (ca. 2 g) firmly glued to one end of the beam. Meanwhile, in order to simulate the damping forces acting on the beam, the straw was inserted into a cup of viscid fluid during the experiments. The depth of submersion was set in such a way that the straw was at the depth d when the beam at its static equilibrium position. For example, in the case of d = 0 mm, the tip of the straw was just about to contact the liquid surface before the beam started oscillating. On the other hand, the tip completely immersed inside the viscid fluid during the oscillations if d = 30 mm or larger. Since the damping force is proportional to the depth inside the liquid, the straw thus was to mimic the attractive and repulsive forces acting to the cantilever from the tip of probes. Refer to Fig. 4 the details of the setup.

During the experiments, the sampling frequency f_s was set to 200 Hz. And, sinusoidal excitations with the constant frequency (Ω) were applied from the controller to the shaker and detected by accelerometer 1 (S1, DYTRAN Model 3136A), which directly mounted on the base of the cantilever. The amplitudes of these excitations were all kept the same while its frequency may be changed if so desired. The system responses were then detected and acquired by accelerometer 2 (S2, DYTRAN Model 3031B, wt. 5.5 g), which was located at the free end of the beam ca. 186 mm from its fixed point. Both signals were then acquired and sent to a laptop computer for the later analyses.

The equivalent flexural stiffness of the current test specimen, modeled as a cantilever beam, may be found from fundamental textbooks, or

$$k_t = \frac{3EI}{\ell^3} = \frac{3\times 210{,}000\times \frac{20.2\times(1.6)^3}{12}}{(186)^3} = 0.675 \ \ (\mathrm{N/mm})\,.$$

And, it has been noted as Case 6 in Table 2. In addition, the deflections of the specimen were measured by putting on static loads at the location of ca. 240 mm from the fixed point from the former experiments. From those static deflection measurements, the spring stiffness has been obtained: $k_{s240} = 0.369$ N/mm. That is equivalent to $k_s = 0.793$ N/mm at $\ell = 186$ mm, shown in Table 2 as Case 7. Having the information and set-up *a priori*, the dynamic experiments started carrying out. The beam specimen was excited by a chirp since signals and found ω_0 for five different damping conditions. The liquids are air, SAE #40 and #300 oil with various depths d, which are shown as Case 1 to 5 in Table 2. Note also that the so-called Fourier Coefficient method, that uses the Fourier coefficients of the product modulation of inputs $u(t)$ and its output $z(t)$, given in [20] has been adopted for the calculation of the dissipative energy. A typical modulated signal in the frequency domain is shown in Fig. 5. Referring Fig. 5, notice also that the Fourier coefficient $\alpha_2 \gg a_0$ even though coefficient a_0 is not exact zero. In fact, coefficient a_0 here also plays as a role for checking whether ϕ is right at $\pi/2$. In case ω_0 is correctly located, coefficient a_0 should be very close to zero.

The spring constant calibration for the probe cantilever is executed as soon as it is mounted onto the clip. Or, it is normally performing in air, which is shown in Table 1 as Case 1. Referring Table 1, it showed that the estimated stiffness ($\hat{k}$) of cantilever beam has its spring constant 0.7019 (SD: 0.031) N/mm, or the 90% confidence interval ranges from 0.6451 to 0.7586 N/mm. The upper or lower bound is ca. 8% of its mean value, which stands for quite accurate calibration in comparison with the values from a commercial catalog [e.g., 21, 22]. In addition, the mean spring constant of 0.7019 N/mm is quite reasonable when comparing with k_t and k_s which are 0.657 and 0.793 N/mm, respectively. From this result, one can confidently concludes that the present method can identify the spring constant of the cantilever beam with good accuracy. Without a doubt, it can be further applied to calibrate the spring constant of every single probe after it is mounted on the probe holder clip.

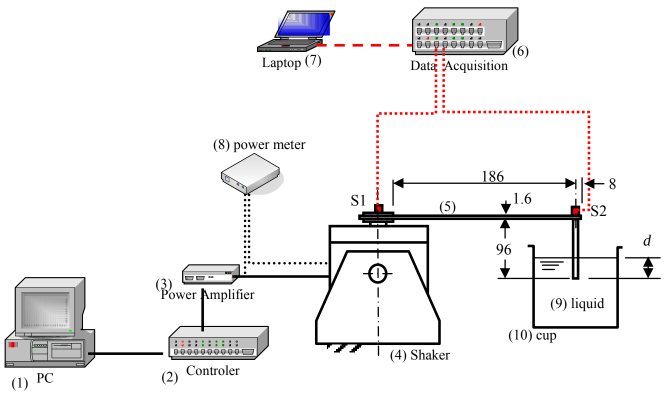

Fig. 4. The experimental set-up (1: PC; 2: signal controller, Dactron; 3: Power Amplifier, B&K 2706; 4: Exciter, B&K 4809, 5: Cantilever; 6: Acquisition system, iMC μ-Musys; 7: PC and Software, FAMOS; 8: Power meter; 9 & 10: damper and liquid).

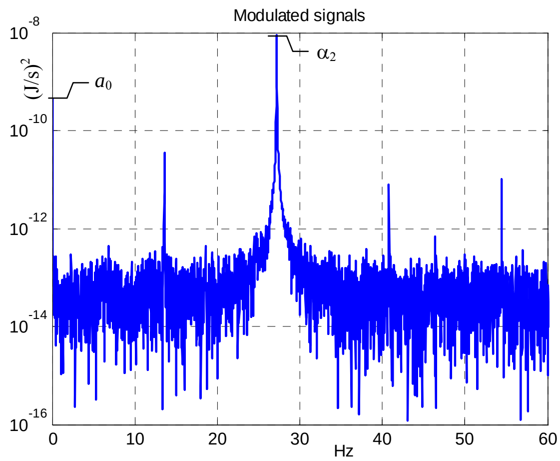

Fig. 5 FFT for a typical modulated signal $g(t) = z(t)\cdot u(t)$ at Ω = 14.1 Hz.

In addition to Case 1 for the spring constant calibration, several damping situations using the mentioned viscid fluids have been also given. Notice from Table 2 on Case 2 and 3, in which the free end of the straw on the cantilever tip was completely immerse inside the liquid during oscillations.

Under these circumstances, a large damping at the straw tip was simulated. That is, the dissipative energy from the straw might be much higher than that of from the beam itself. As a consequence, the present method recognized a lower spring constant for the beam. Furthermore, similar to the results of numerical simulations presented in the last section, low quality factors have been noticed that may also include some error from other sources as well.

Table 2 Comparisons of identified spring constants

	Case ID	liquid	d (mm)	$\hat{k}$ (SD) N/mm	Remarks
dynamic	1	--	--	0.7019(0.0310)	$\hat{Q} \doteq 26.50$
	2	#40 oil	30	0.6018(0.0152)	$\hat{Q} \doteq 6.56$
	3	#300 oil	30	0.6257(0.0159)	$\hat{Q} \doteq 5.24$
	4	Air/oil#40	≈ 0	0.7888(0.0143)	
	5	Air/oil#300	≈ 0	0.7930(0.0162)	
static	6	--	--	0.6750	$k_t = 3EI/\ell^3$ @ $\ell = 186$ mm
	7	--	--	0.7930	k_s @ $\ell = 186$ mm

* SD = Standard Deviation.

Case 4 and 5 shown in Table 2 represent two strongly nonlinear damping systems. The straw was set slightly above the viscid fluid surface when it was in its static equilibrium. When the beam started oscillating, one half of the straw oscillation stays in the liquid while the other half in air. The former half in fluid stands for a strong damping, while the latter one for weakly damped. Even though the identified results shown in the table are still quite reasonable, the possible reason may originate from that the present method is actually evaluate the equivalent dissipative energy [18]. It does not matter if the energy is initiated from linear or nonlinear damping. How-ever, it has been found that the main error source of these experimental measurements were from determining the location of ω_0. This situation also implies that a robust control algorithm may be needed in case of systems with strongly nonlinear damping. Nevertheless, the experimental results once again confirmed that the present identification method can successfully detect the spring constant of a cantilever beam which mimics the probe of AFMs. However, more studies on real AFM probes may be still desired.

CONCLUDING REMARKS

A new identification method has been derived for sdof, base-excited systems. The system is to mimic a cantilever probe system of AFMs. In fact, the idea of the present report was initiated by needs for *in situ* spring constant calibration for the probe systems. Such a calibration process can be treated as parameter identification for the stiffness of each probe before it is used. However, sine a real probe is too small and costly to verify, a cantilever beam was adopted to replace it during the study. Unlike other existing methods, the present method starts with giving a chirp excitation to the system, and acquires the corresponding responses that are then used to lock the damped natural frequency of the beam. Once the damped natural frequency is obtained, it is possible to compute the frequency location where the phase lag is equal to $\pi/2$ (or 90°) by using the formulation given in the present report. From which, the present calibration process is to require the external excitation frequency purposely changes to that frequency and the steady-state responses are stored for the later analyses. In the meantime, the system dissipative energy or power may also be experimentally measured for estimation of the probe damping.

In fact, the present identification formulation is to express both the stiffness of the target probe in terms of two directly measurable parameters. They are the phase angle as well as system damping. The former can be computed from the damped natural frequency and then used to locate the input excitation frequency of steady-state responses. On the other hand, the latter can be identified along with measuring the input power since the equivalence of the dissipated and input energies when the system oscillations are in steady-state.

After the theoretical derivation, the report also provided numerical simulations using the Simulink toolbox of MATLAB. Depending on the error of the quality factor, which is a function of the probe damping, the simulated results clearly showed the current identification method can work with good accuracy. Following the numerical simulation, experimental measure-ments were also carried out by a cantilever beam that its free end was immersed to viscid fluids. Fluids of different viscosity were used to imitate the environments of a probe in use. The experimental results again substantiated the validity of the method. Thus it is accordingly concluded that the new recognition algorithm can be applied with confidence. In addition, one summarizes the whole calibration procedures as follows:

(1) Apply a chirp or wide-band signal to scan the location of the damped natural frequency of the target system as well as the quality factor of the system.
(2) Use the formulations given in (11) and (12) to compute the frequency location where the phase angle equals to 90°. Denote that frequency as ω_0.
(3) Apply external excitation again to the target system but with the frequency right at ω_0.
(4) Acquire the steady-state responses, both input and output. In case power meter is available, it is recommended to measure the dissipative power simultaneously.
(5) Utilize the equations given in the present report and compute the corresponding spring constant of the system.
(6) Repeat the former steps for checking.

ACKNOWLEDGMENTS

The present research is partly supported by National Science Council (NSC) of Taiwan under No. NSC 97-2212-E-027-027. The first author owes his deepest gratitude to NSC. Besides, the experimental verification was performed by Mr. Jung J. Tsai and Ren L. Lin. The authors are also grateful to their contributions.

REFERENCES

[1] Burnham, N.A. et. al, 2003, "Comparison of calibration methods for atomic force microscopy cantilevers," Nanotechnonogy, 14, pp. 1-6.

[2] Gibson, C.T., Weeks, B.L., Abell, C. Rayment, T., Myhra, S., 2003, "Calibration of AFM cantilever spring constants, Ultramicroscopy," pp. 113-118, 97.

[3] Poogi, M.A., McFarland, A.W., Colton, J.S., Bottomley, L.A., 2005, "A method for calculating the spring constant of atomic force microscopy cantilevers with a nonrectangular cross-section, Analysis Chemistry," 77, pp.1192-1195.

[4] Shaw, G.A., Kramar, J., and Pratt, J., 2006, "SI-traceable spring constant calibration of microfabricated cantilevers for small force measurement," Experimental Mechanics, DOI 10.1007/s11340-006-9394-9.

[5] Sader, J.E., Pacifico, J., Green C.P., Mulvaney, P., 2005, "General scaling law for stiffness measurement of small bodies with applications for the atomic force microscope, J. Applied Physics," 97, pp. 124903-124907.

[6] Hutter, J.L and Bechhoefer, J., 1993, "Calibration of atomic-force microscope tips, Review of Scientific Instruments," 64(7), pp. 1868-1873.

[7] Butt, H-J., and Jaschke, M., 1995, "Calculation of thermal noise in atomic force microscopy," Nanotechnology, 6, 1-7.

[8] Cleveland, J.P., Manne, S., Bocek, D. and Hansma, P.K., 1993, "A nondestructive method for determining the spring constant of cantilevers for scanning force microscopy," Review of Scientific Instruments, 64(7), pp. 403-405.

[9] Salehi-Khojin, A., Bashash, S., Jalili, N., et al., 2009, "Nanomechanical cantilever active probes for ultrasmall mass detection," Journal of Applied Physics, 105 (013506), 2009.

[10] Jericho, S.K. and Jericho, M.H., 2002, "Device for the determination of spring constants of atomic force microscope cantilevers and micromachined springs," Review of Scientific Instruments, v. 73, pp. 2483-2485, (6).

[11] McClure, P.F. and Mancevski, V., 2005, "Calibration of a dual probe NanoCaliper AFM for CD metrology," Proc. Of SPIE, v. 5752, pp.922-936.

[12] Gibson, C.T., Watson, G.S. and Myhra, S., 1996, "Determination of the spring constants of probes for force microscopy/spectroscopy," Nanotechnology, 7, pp.259-262.

[13] Sader, J.E., Larson, I, Mulvaney, P. and White, L.R., 1995, "Method for the calibration of atomic force microscope cantilevers," Review of Scientific Instruments, 66(7), pp. 3789-3798.

[14] Stark, R.W., Drobek, T., and Heckl, W.M., 2001, "Thermomechanical noise of a free V-shaped cantilever for atomic force microscopy," Ultramicroscopy, 86, pp. 207-215.

[15] Levy, R., and Maaloum, M., 2002, "Measuring the spring constant of atomic force microscope cantilevers: thermal fluctuations and other methods," Nanotechnology, 13, pp. 33-37.

[16] Holbery, J.D., Eden, V.L., Sarikaya, M., and Fisher, R.M., 2000, "Experimental determination of scanning probe microscope cantilever spring constants utilizing a nano-indentation apparatus," Review of Scientific Instruments, 71(10), pp. 3779-3776.

[17] Li, W., 2005, "Evaluation of the Damping Ratio for a Base-excited System by the Modulations of Responses," J. Sound and Vibration, 279, pp. 1181-1194.

[18] Li, W., Chang, C.W., and Tseng, S. P., 2006, "The linearization method based on the equivalence of dissipated energies for nonlinearly damped structural systems," J. Sound and Vibration, 295, pp. 797-809.

[19] Li, W., Lin, R. L., and Liu, C.W., 2006, "The study of a power detector circuit for the Probe of Atomic Force Microscopes," Proc. PMMT-2006, E39-01~E39-08, (in Chinese).

[20] Li, W., 2007, A method to measure the dissipative energy of structural damping, Taiwanese Patent No. I 283740.

[21] Nano Sensors website: http://www.nanosensors.com/CNT-FM.htm.

[22] Budget Sensor website: http://www.budgetsensors.com/tapping_mode_afm_probes.html.